ChemMedChem

Concept
doi.org/10.1002/cmdc.202300296

Chemistry Europe
European Chemical Societies Publishing

www.chemmedchem.org

Water-Soluble Fullerene Monoderivatives for Biomedical Applications

Rohin Biswas,[a] Cassiana Batista Da Rocha,[a] Ryan A. Bennick,[a] and Jianyuan Zhang*[a]

Monoderivatives of fullerenes functionalized with hydrophilic groups make them water soluble, while preserving the hydrophobic fullerene cage. This class of molecules have intriguing biomedical applications, including drug delivery, photodynamic therapy (PDT), antiviral and antimicrobial activity and reactive oxygen species (ROS)-scavenging abilities. In this Concept we discuss the synthesis and biomedical applications of water-soluble fullerene monoderivatives and their biological behavior based on their structures.

Introduction

Water-soluble fullerene derivatives are useful building blocks for biomedical applications.[1,2] However, the inherent structures of these molecular scaffolds are highly hydrophobic,[3] which can pose a challenge towards their use in biological systems as water-solubility is often a prerequisite for medicines. Functionalization of the fullerene cage has yielded many water-soluble derivatives which contain multiple hydroxyl, carboxyl or amino hydrophilic groups;[4–7] however, with the exception of $C_{60}(OH)_{8}$,[8] these derivatives have imprecise structure and batch-to-batch variations. On the other hand, precise functionalization of fullerenes can be realized by the synthesis of monoadducts which have already been used for a broad range of applications such as energy, diagnostics and therapeutics.[2,9,10] For example, fullerene monoderivatives have been widely used in organic solar cells[11,12] and perovskite solar cells.[9] In our Concept article, we will discuss water-soluble fullerene monoderivatives for biomedical applications, with the highlights on these directions: cellular uptake of functionalized fullerene monoderivatives; leading to their anticancer activity and ability to be effective photosensitizers for PDT, antiviral and antibacterial activities and ROS scavenging.

A few widely-used cycloadditions, including Bingel-Hirsch, Prato, and Diazo addition reactions, to synthesize monoadducts of fullerenes had been established in the 1990s,[13,14] and radical reactions are also available to functionalize fullerenes.[15] These reactions have led to many biologically useful fullerene monoderivatives. Broadly, on the basis of structure, they have been divided into two wide categories – Prato monoadducts (Figure 1) and cyclopropanation (Bingel-Hirsch and other 3-membered rings) adducts (Figure 2). The 1,3-dipolar Prato reaction is versatile to introduce various hydrophilic functional groups to bestow the fullerene water-solubility. Additionally a positively charged nitrogen in a fulleropyrrolidine group such as those shown in (Structures 1, 2 and 4) can impart water-solubility as well. Moreover, other water-soluble Prato monoadducts containing a net charge (Structures 5, 8, 10, 12, 14 and 15) and those that are uncharged (Structures 3, 6, 7, 11, 13, 16 and 17) have also been depicted in Figure 1.

In Figure 2, the 3-membered ring based monoadducts can be categorized as several kinds. Monoderivative 18, is the first reported water-soluble C_{60} monoderivative to be used to inhibit HIV enzymes.[16,17] Structures 19 and 20 are examples of monoadducts containing peptides. Structures 21–25 are saccharide derivatives of C_{60} with 22–24 being typical Bingel-Hirsch derivatives. Structures 25 and 26 are direct additions of azido groups on the fullerene cage. In addition to structural precision, another important advantage of fullerene monoderivatives is that the functionalization preserves the hydrophobic cage which makes them amenable for drug delivery, ROS-scavenging, and immunological properties.[2,18–21]

Cellular uptake, anticancer activity and photosensitizer behavior of fullerene monoderivatives

A key requirement for a functional fullerene monoderivative to exert its biological activity is good cellular uptake. With that said, in most cases, cellular uptake alone is insufficient for the desired biological outcome; rather, targeting of the molecules to specific sub-cellular locations such as certain cell organelle(s) may be necessary.[22] Several reports have shown the enhanced cellular uptake of the conjugate due to the presence of a hydrophobic fullerene in the structure. For instance, a water-soluble fullerene monoderivative, $C_{61}(CO_2H)_2$ had high cellular uptake and selectively localized in the mitochondria of COS-7 cells.[23] A study by Yang et. al. demonstrated that a fullerene peptide conjugate had higher cellular uptake than without the fullerene;[24] and in a follow-up work by the same group, Zhang

[a] R. Biswas, C. Batista Da Rocha, R. A. Bennick, Dr. J. Zhang
Department of Chemistry and Chemical Biology, Rutgers
The State University of New Jersey
123 Bevier Road, Piscataway, NJ 08854 (USA)
E-mail: jy.zhang@rutgers.edu

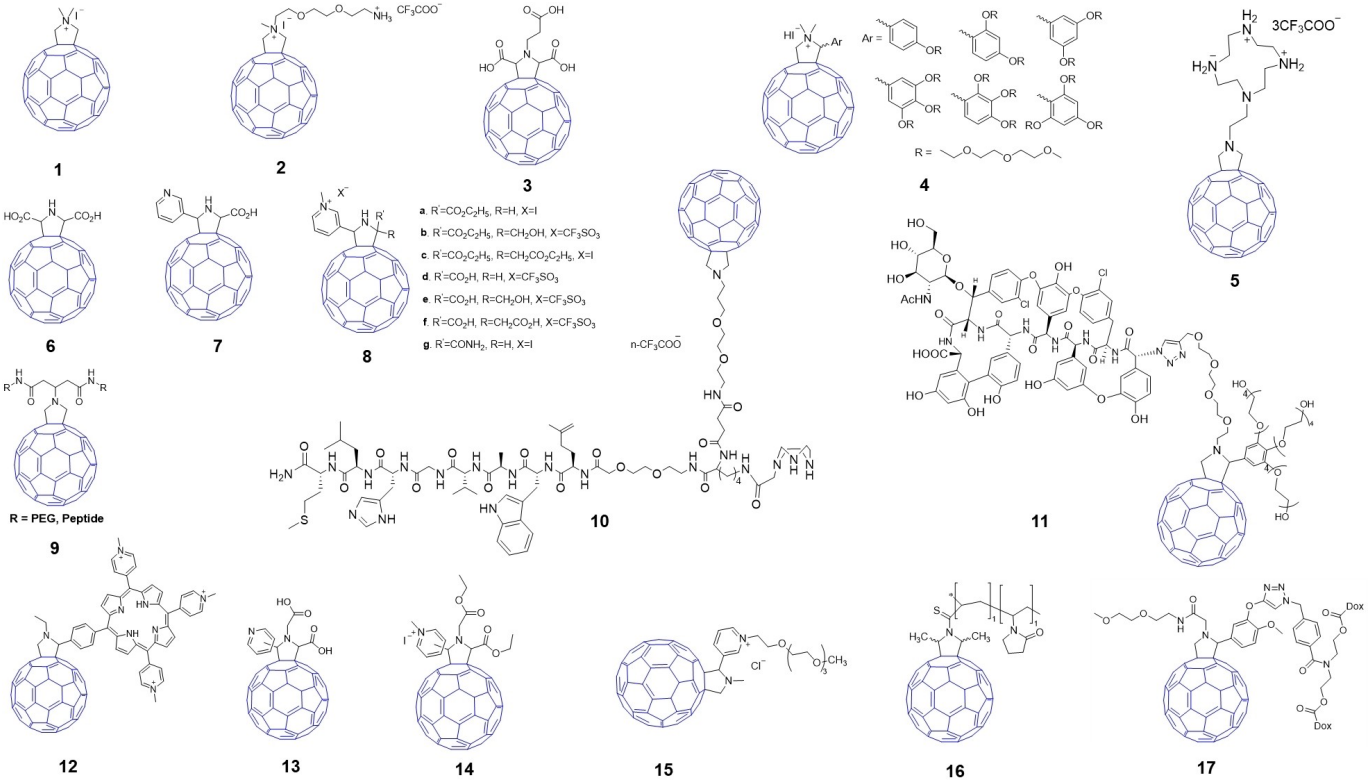

Figure 1. Examples of water-soluble C_{60} Prato derivatives.

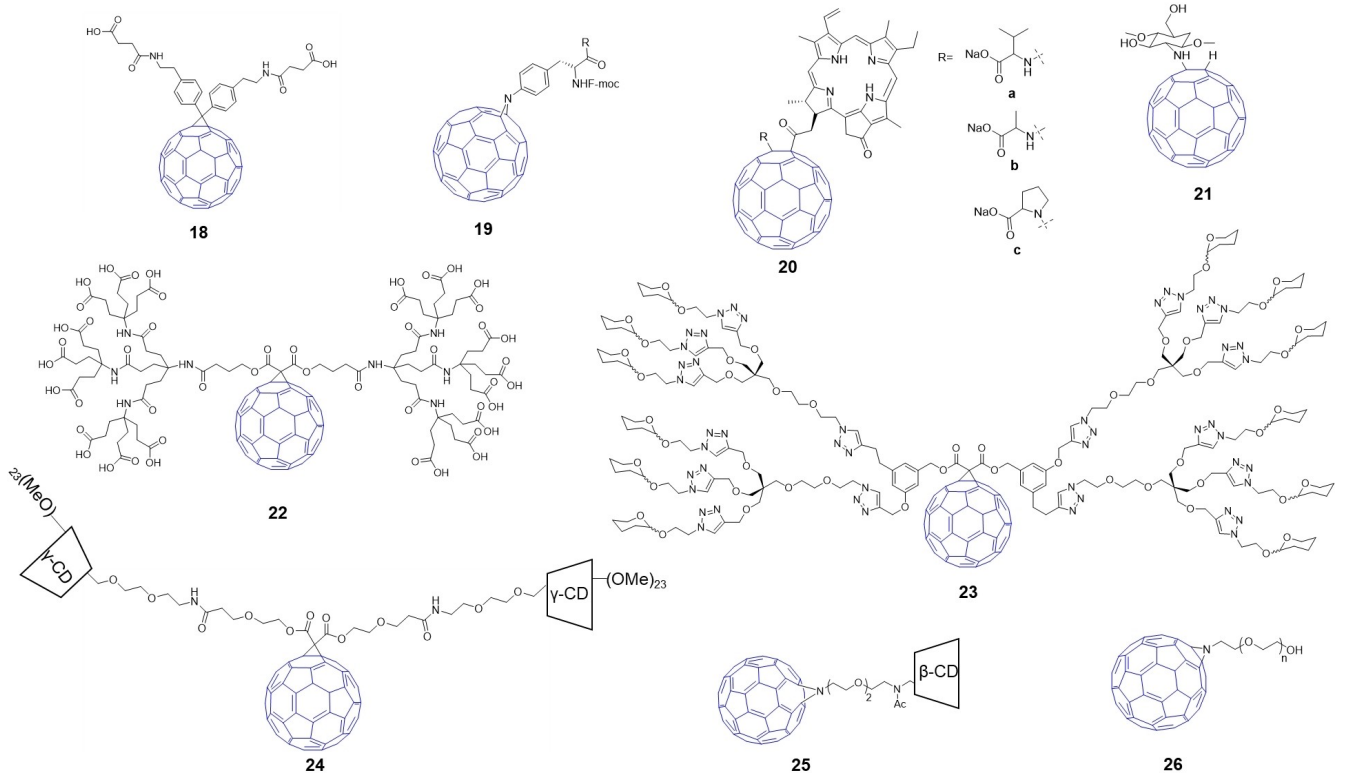

Figure 2. Examples of water-soluble C_{60} Bingel-Hirsch and other C_{60} derivatives.

et. al. discussed the possible endocytic mechanism of cellular uptake of such fullerene peptide conjugates. The authors concluded that the uptake could be mediated by caveolae/lipid rafts and cytoskeletal components. Moreover, localization of the conjugate in the lysosome was not observed.[24,25] Additionally, a fullerene doxorubicin conjugate was found to have high cellular uptake in the cytoplasm of MCF-7 cells suggesting possibility of using fullerenes in delivering small molecule drugs inside cells.[26] PEGylated fullerene doxorubicin conjugates (Figure 1, structure 17) have also been investigated for their anticancer activity.[27]

In another study, a conjugate of fullerene with dextran, C_{60}-Dex-NH_2 was used to deliver siRNA in a controlled manner by using visible light as the stimulus. As with most cargo which get trapped by endosomes, the same was observed for this delivery system which was overcome by ROS mediated damage to endosomes and escape for effective delivery of siRNA in vitro and in vivo.[28] Furthermore, a study by Kobayashi et.al. showed the synthesis of pyridinium-type fullerene derivatives which inhibited HIV enzymes (Figure 1, structures 6–8). As shown in Figure 3, the cellular uptake of the pyridinium/ethyl ester-type derivatives, cis-**3a** (Figure 1, 8a), cis-**3e** (Figure 1, 8b), and cis-**3g** (Figure 1, 8c), were higher than the carboxylic acid or amide type derivatives.[29]

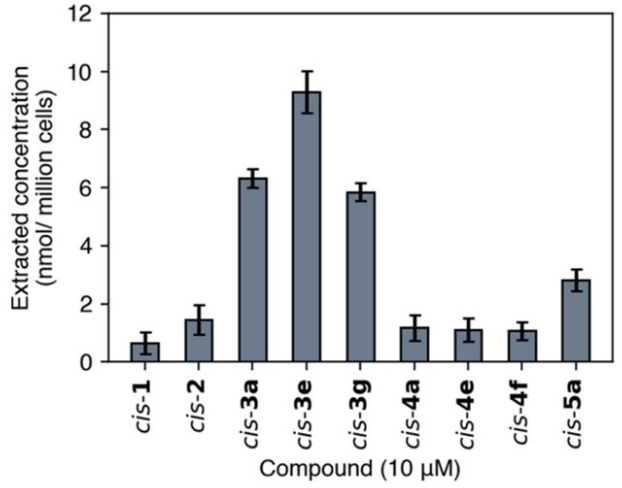

Figure 3. Cellular uptake of fullerene derivatives. Adapted from Ref. [29].

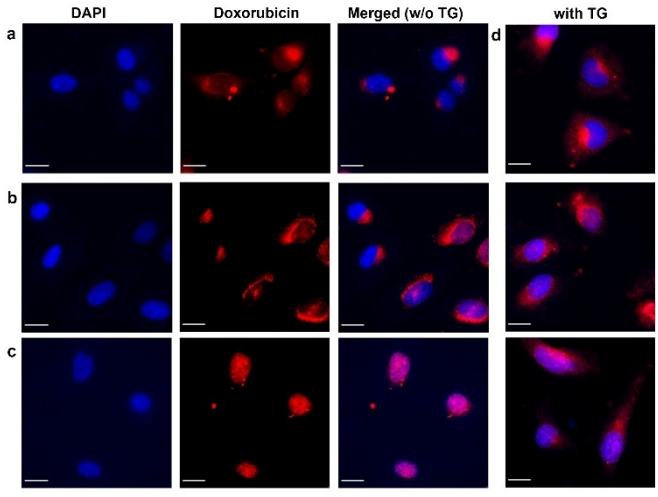

Figure 4. Fluorescence images of HeLa cells treated with doxorubicin (Dox) loaded drug delivery systems. Dox@CD (a), Dox@FCD (b), Dox@hFCD (c). HeLa cells were pre-treated with thapsigargin (TG) followed by treatment with Dox@CD, Dox@FCD and Dox@hFCD (d). Scale bars are 20 μm. Adapted from Ref. [18].

We recently demonstrated a water-soluble C_{60} mono Bingel-Hirsch derivative with specific sub-cellular targeting.[18] A C_{60} monoderivative was conjugated with β-cyclodextrin to yield an amphiphilic molecule, FCD, which was also further hydroxylated to generate a more hydrophilic derivative, hydroxylated FCD or hFCD. Both systems were loaded with doxorubicin to yield Dox@FCD and Dox@hFCD respectively with a control compound Dox@CD without a fullerene. As shown in Figure 4, Dox@CD produced no specific localization of doxorubicin in any organelle in HeLa cells. Dox@FCD on the other hand was found to localize in the lysosome for a significantly longer time and could localize in the nucleus and deliver doxorubicin after a significantly long time (~24 hrs). Dox@hFCD swiftly escaped the lysosomes and delivered doxorubicin inside the nucleus. The difference in behavior between Dox@FCD and Dox@hFCD was attributed to the ability of hFCD to break down into smaller aggregates in acidic lysosomes which FCD could not. Furthermore, as shown in Figure 4d, blocking the nucleus pore complex using thapsigargin significantly reduced the doxorubicin fluorescence in the nucleus in the case of Dox@hFCD, suggesting it to be the dominant pathway for the uptake of such C_{60} derivatives inside the nucleus.[18]

Beyond the structural requirements of the fullerene monoderivatives that the authors have highlighted for their efficient cellular uptake, the functional roles of these fullerene derivatives have been discussed next. Broadly, we mention the anticancer activity of some of these water-soluble fullerene monoderivatives, their mode of causing cellular toxicity either through release of a drug present in the fullerene monoderivative or through its photosensitizer activity such that upon irradiation of light of a specific wavelength, the derivative can generate ROS leading to cytotoxicity to the cancer cell.

A list of the specific functions of some of these fullerene derivatives highlighted in Figures 1 and 2, have been tabulated in Table 1 below.

A promising use of water-soluble fullerene derivatives containing a nearly intact conjugated fullerene cage is in PDT as the photophysical properties of fullerenes make them desirable candidates to be a photosensitizer,[30] as fullerenes can facilitate intersystem crossing (ISC), as discussed in some excellent reviews.[31,32] As a non-invasive technique PDT is a promising therapeutic modality for cancer,[33] as demonstrated in the work by Guan *et. al.*[34] As shown in Figure 5, in the presence of C_{70}, the conjugate PC_{70} showed higher reduction in cell viability of A549 cells compared to the control compound, D-TMPyP which lacks C_{70}. The importance of fullerene was further corroborated by the cell images where upon treatment with PC_{70} followed by light irradiation led to severe damage to

Table 1. Summary of anticancer and photosensitizer activities of some fullerene monoderivatives highlighted in Figure 1 and 2.

Structure	Reference	Cellular uptake	Quantum yield	Cytotoxicity induction mechanism
1	[37,38]	Liposome loaded with 1 underwent effective endocytosis due to electrostatic interactions		Photoirradiation leading to cytotoxicity in HeLa cells
2	[40]			Cell death by apoptosis by increasing the eATP activated P2X7R pathway in macrophages.
15	[43]	Electrostatic interaction; positively charged derivative interacted with cell membrane		ROS (singlet oxygen) mediated cytotoxicity was observed in A549 cells.
17	[27]	Lysosomal accumulation after endocytosis		Cytotoxicity mediated by released doxorubicin, possibly by already known mechanisms of doxorubicin toxicity in MCF-7 cells.
20	[45]		20a: 4.6×10^{-3} 20b: 3.5×10^{-3} 20c: 9.4×10^{-3}	Phototoxicity in HeLa cells for all the three derivatives through Type 1 ROS generation (superoxide radical).
21	[46]	Cellular uptake observed although no mitochondrial uptake although ROS was generated in mitochondria		ROS mediated photo cytotoxicity observed in A549 cells when treated with fullerene conjugate.
24	[47]		0.27 ($^1O_2$)	
25	[48]	Readily internalized by cells, in tumor bearing mice distribution observed in heart, liver, kidney, stomach, intestine, brain and spleen		Dose-dependent photo-cytotoxicity against SH-SY5Y cancer cells due to ROS generation by the fullerene derivative primarily through hydroxyl and superoxide radical generation.

the cells under anaerobic conditions. In another report by Tang *et. al.*,[35] the authors synthesized a C_{60}-rhodamine conjugate, C_{60}-RB. Under acidic conditions the conjugate got activated with an enhancement of visible light absorbance together with fluorescence turn-on and triplet excited state generation. This led to a reduction in the energy gap between the singlet and triplet excited states to 0.017 eV which ensured good intersystem crossing (ISC) with strong PDT activity in HCT-116, HeLa, A2780 and A549 cells. Furthermore, in a recent article by Lopez *et. al.*[36] a C_{60}-BOPHY conjugate was found to photoinactivate microbes like *S. aureus* and *E. coli* through an efficient energy/electron transfer process from BOPHY to C_{60} and it was found that the conjugate had a higher efficacy as a photosensitizer than either of the components.

In addition to the above examples, compounds 1 and 3 (Figure 1) were found to generate ROS making them effective photosensitizers. Additionally, compound 3 was shown to have sonodynamically activated antitumor effect[37–39] while compound 2 was found to have good immunological properties.[40] Compound 10 in Figure 1 while couldn't be isolated in substantial amount, showed strong PDT potential.[41] Some of these compounds have been highlighted in a previous review.[2] Here we highlight Prato monoderivatives shown in Figure 1 with photosensitizer properties such as structure 12, a porphyrin derivative with DNA cleavage activity,[42] structure 15 with strong photosensitizing activity in A549 cells and a polymeric fullerene derivative with extremely high water-solubility that caused superoxide radical mediated DNA damage.[43,44] Other chromophores such as pyropheophorbide linked to amino acids (Figure 2, structure 20) have been used as photosensitizers showing Type 1 ROS mediated phototoxicity in HeLa cells.[45] Endogenous ROS generated in mitochondria by a C_{60} chitosan conjugate shown in Figure 2, structure 21 showed promising photodynamic therapy in A375 cells.[46] Fullerene derivatives containing one or two cyclodextrins have also shown potential as effective photosensitizers as pointed out in Table 1.[47,48]

Interestingly, the photophysical behavior of fullerene monoderivatives has profound dependence on their molecular structure. In the work by Liosi *et. al.*[19] C_{60}-PEG and C_{70}-PEG monoadducts synthesized via Prato reaction (Figure 6a) were tested for their ability to generate ROS under visible light irradiation and cause photoinduced DNA damage. The authors synthesized three fullerene monoderivatives (Figure 6a), C_{60}-PEG1, C_{70}-PEG2, and C_{70}-PEG3, and the difference between the two C_{70} monoderivatives were the functionalization site being either on the ab bond near the "tip" of C_{70} or the cc bond slightly closer to the middle. The study revealed a clear difference in the preference for ROS generation between C_{60}-PEG1and the two C_{70}-PEG monoadducts. In the presence of NADH, an electron donor, $O^{2\bullet-}$ generation was highest for C_{60}-PEG1 as shown in Figure 6b, suggesting a *type I* pathway which partially correlates to the percentage of nicked DNA. Further shown in Figure 6c, is the amount of $^1O_2$ generated through *type II* pathway using 4-oxo-TEMP as spin trap showing that C_{70}-PEG2 predominantly acts as a photosensitizer via the *type II* pathway. The disparity in pathways was dependent on the fullerene core (C_{60} or C_{70}) and the functionalization pattern. C_{60}-PEG1 had a higher preference for *Type I* pathway whereas C_{70}-PEG2 with the *ab*-[6,6] addition site preferred the *type II* pathway. These findings provide insights for optimizing param-

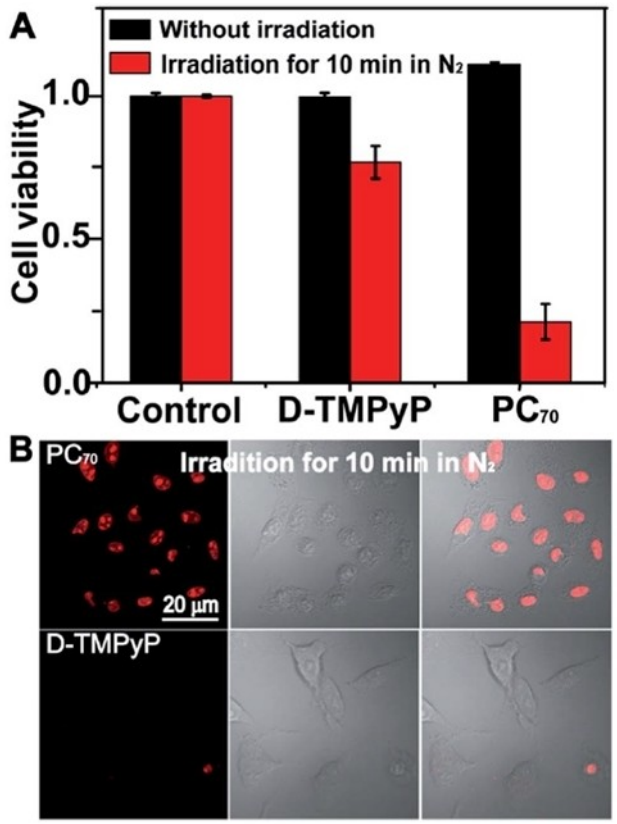

Figure 5. Cell viability of A549 cells incubated with either PC70 or D-TMPyP for 3 h and subsequent irradiation for 10 min at a power density of 17 mW cm-2 under nitrogen. Cells without irradiation were used as a control. (A) Confocal images of A549 cells stained with PI after treatment with 2 mM PC_{70} for 3 h and subsequently exposed to light irradiation for 10 min at a power density of 17 mW cm-2 under nitrogen. Cells treated with D-TMPyP were used as a control.(B) Adapted from Ref. [34].

eters like excited states lifetime, redox potential, and electron transfer rate for the development of efficient new PDT-photosensitizers based on fullerene derivatives.

The close relative of fullerenes, endohedral metallofullerenes (EMFs),[49] were also solubilized in an analogue of monoderivative approach. EMFs are safe carriers of metal ions,[50,51] but like fullerenes, their water-soluble derivatives are typically imprecise. Through exohedral functionalization using established reactions for EMFs,[52,53] we demonstrated a "metallobuckytrio" (MBT) system, shown in Figure 7a, where precise monoderivatives of EMFs $Lu_3N@C_{80}$ and $Gd_3N@C_{80}$ were connected to a C_{60} core bearing hydrophilic ligands.[54] Our modular approach provide structurally defined Gd MBTs which as seen from Figure 7b are excellent MRI contrast agents. When compared with gadodiamide, a commercially used contrast agent, our Gd MBTs at the similar concentration of gadodiamide provided a much higher contrast in MRI (Figure 7b). Because there is no water molecule directly coordinated with the Gd ion, and there is no hydroxyl groups attached to the EMF cage, the higher relaxivity values are likely resulted by the large aggregation size of the molecules, thanks to their amphiphilic nature. Also, the conjugated structure of the C_{60} core and the EMF cage contributed to ROS generation under green light irradiation, making the MBTs potential candidates for PDTs.

The above mentioned studies provide important structure-function insights of the requirements for biocompatible fullerene derivatives,[55,56] their enhanced cellular uptake and subcellular targeting of fullerene monoderivatives. The importance of a hydrophobic structure such as a fullerene cage, to enhance cellular uptake, is evident when higher efficacy of conjugates containing a fullerene was observed inside cells.[18,24] To understand the definitive cellular behavior of fullerene monoderivatives which can be correlated to the surface functionalization for better future designs, a direct visualization of these conjugates inside cellular compartments is highly desirable, which can be realized by conjugation of fluorophores to the fullerene monoadducts. Additionally, when looking at photosensitizer behavior of water-soluble fullerene derivatives, it is evident that a relatively conjugated fullerene cage is essential for ROS generation such as that in a fullerene monoderivative compared to higher derivatives where the fullerene cage loses its conjugation, however in aqueous solution the monoderivatives have a strong tendency to form large aggregates which can often be detrimental to their effectiveness in acting as a photosensitizer. Hence, monoderivatives having a net charge may be desired to prevent such aggregation and yet have good photophysical properties.

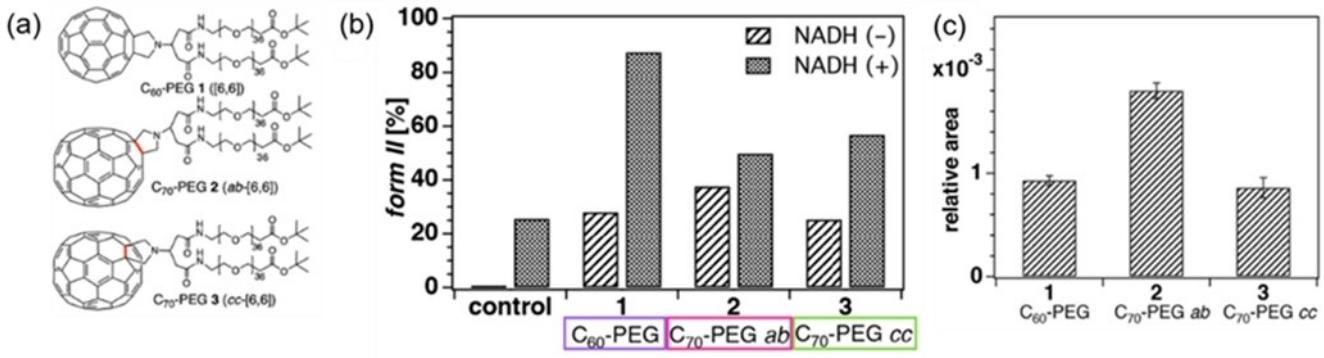

Figure 6. Fullerene PEG monoadducts (a), photoinduced DNA cleavage showing relative formation of nicked form II (b), relative amount of singlet oxygen generation (c). Adapted from Ref. [19].

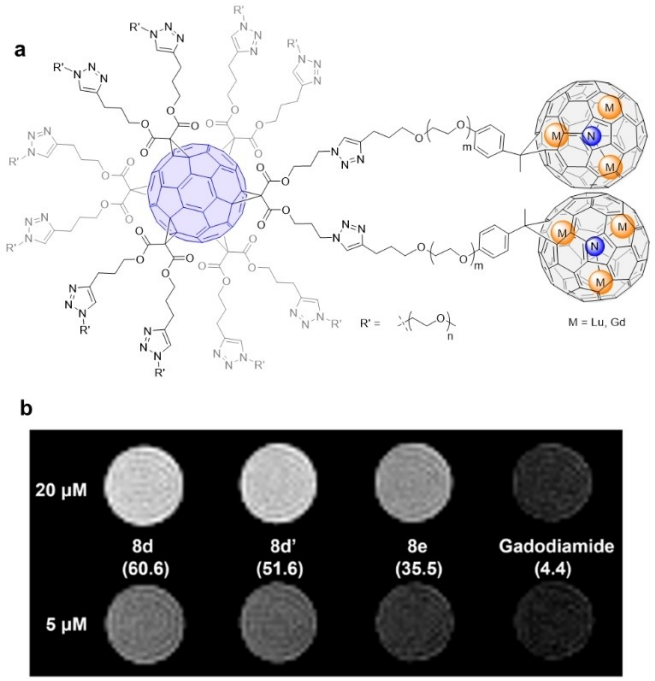

Figure 7. Representative structure of a metallobuckytrio (MBT) system (a), MR imaging of Gd MBT solutions on a 1.0 T scanner. The measured r1 values at 1.4 T are written in parentheses under each compound, in the unit of mM-1s–1. (b). Adapted from Ref. [54].

Antiviral and antibacterial properties of fullerene monoderivatives

With the rise of pathogen related diseases and morbidities such as the Ebola virus outbreak in 2014 and the recent COVID-19 pandemic, there is an increasing demand for antiviral and antimicrobial compounds to combat these deadly diseases. Fullerene monoderivatives have been long used for such purposes. For instance, fullerene monoderivatives have been used to combat the human immunodeficiency (HIV) virus by acting as enzyme inhibitors of HIV such as inhibiting HIV-reverse transcripstase (HIV-RT) by structures 13 and 14 shown above and HIV protease (structure 19) as well as both HIV-RT and HIV protease (structures 18 and 22).[17,57–59] Several such fullerene derivatives for inhibiting HIV enzymes have been reviewed in detail by Echegoyen *et. al.*[2] Munoz *et. al.* demonstrated the ability of a glycodendrofullerene (Structure 23) to act as inhibitor of DC-SIGN, a receptor used by the Ebola virus to induce infection.[60] In addition to anti-viral properties, fullerene monoderivatives having antibacterial activity have been reported, such as structure 5, a fullerene cyclen derivative showed anti-bacterial activity towards *E. coli* and *S. aureus*.[61] Additionally, a fullerene glycopeptide (teicoplanin) conjugate, Structure 11, showed antibacterial behavior towards *E. foecalis* resistant to teicoplanin.[62] These properties of water-soluble fullerene derivatives and their mechanism of pathogen inhibition have been summarized below in Table 2.

From the properties of the above discussed water-soluble fullerene monoderivatives, the following structure-activity relationships can be drawn. Firstly, the fullerene itself can cause membrane stress or block access to the active site of an enzyme. Multivalent systems based on the fullerene scaffold can block the receptor involved in pathogen entry to the target. Additionally, fullerene derivatives with a net charge can also cause membrane depolarization leading to their anti-microbial effect.

Table 2. Antiviral and antibacterial properties of some fullerene monoderivatives shown in Figure 1 and 2.

Structure	*Reference*	*Pathogen targeted*	*Mode of pathogen inhibition*
5	[61]	*Escherichia coli*, *Staphylococcus aureus*	Membrane stress through direct physical contact.
11	[62]	*Enterococcus foecalis*	Multivalency of conjugate overcame known resistance mechanism towards glycopeptides.
13	[57]	HIV	Inhibition of HIV-RT by pyridinium containing fullerene derivatives demonstrating that the presence of fullerene core is important for this activity.
14	[57]	HIV	Inhibition of HIV-RT by pyridinium containing fullerene derivatives demonstrating that the presence of fullerene core is important for this activity.
18	[17]	HIV	Inhibited HIV protease and HIV–R1 and HIV–R2 in low micromolar range, non-toxic to cells.
19	[58]	HIV	Fullerene peptide derivatives inhibited HIV protease at nM concentration range.
22	[59]	HIV	HIV protease and RT inhibition at low μM range. Hydrophilic side arms protrude from the hydrophobic cavity of HIV-protease. Fullerene sphere blocks access to HIV-protease active site where it resides.
23	[60]	Ebola	Inhibits viral infection in a Jurkat cell model by blocking DC-SIGN in the nM concentration range.

ROS scavenging by fullerene monoderivatives

Although fullerene derivatives can promote ROS generation under light illumination as mentioned above, in dark conditions, they can also show strong antioxidative properties by scavenging ROS. The antioxidative behavior can be due to the properties of the functional moiety appended to the fullerene or the unsaturated nature of the fullerene cage which can directly interact with ROS and scavenge them or a combination of both.[63] Fullerene derivatives with strong ROS-scavenging activity has been extensively highlighted in a recent review and earlier works.[5,64–67] Fullerene monoderivatives, as shown in Figure 8, have also shown great promise as efficient ROS scavengers as described in the work by Enes *et.al.* The authors synthesized a series of C_{60} flavonoid conjugates using the Bingel-Hirsch reaction that were found to have high antioxidant behavior under reduced partial pressure of oxygen which was attributed to the synergistic ROS-scavenging ability of fullerene and the flavonoid moiety on the cage whereas the peroxide radical trapping efficiency in air-saturated solutions was dictated by the phenolic moiety in the structure.[20] Furthermore, Zhao *et. al.* has reported that conjugating a dipeptide to C_{60} enhanced antioxidant activity of the conjugate by 20–30% under peroxyl radical-induced oxidation of DNA as the C_{60} could facilitate intercalation of the dipeptide into the DNA strands which improved the antioxidant capacity of the molecule and inhibited oxidation of DNA.[21] Additionally, Prato monoadduct, Structure 2 was found to induce ROS-scavenging activity in MDM-LPA cells when subjected to oxidative stress.[40] Furthermore, another Prato monoadduct, Structure 4 bearing different number of PEG groups showed hydroxyl radical quenching, specifically the derivative bearing PEG groups at the 2,3,4 position on the benzene ring.[68]

Structure-property analysis of water-soluble fullerene monoderivatives with respect to their ROS-scavenging activity tells us that the presence of a conjugated cage is important to scavenge the radical species, however the functional groups on the fullerene can strengthen the ROS-scavenging capacity. Conjugated systems functionalized to the fullerene such as benzene rings in structures **4** and those shown in Figure 8 could improve this behavior further. More importantly, water-soluble groups added post functionalization can tune the aggregation of these monoderivatives in aqueous solution due to their amphiphilic nature which can further influence their ROS-scavenging activity.

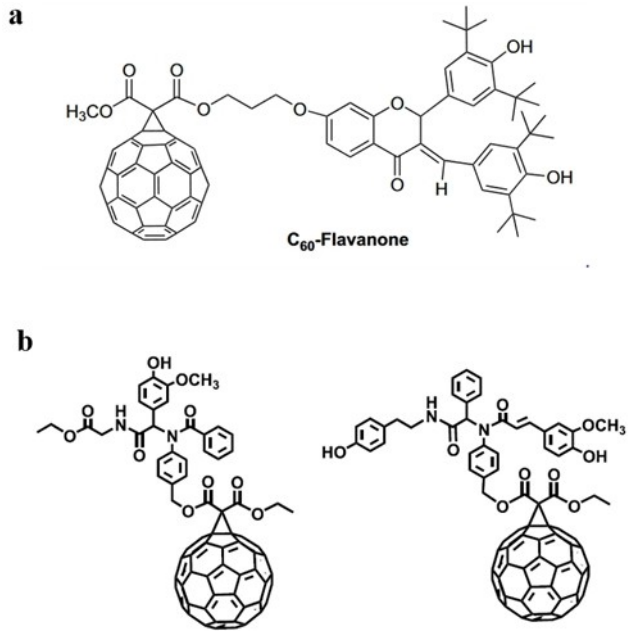

Figure 8. Fullerene derivatives with strong ROS-scavenging activity; fullerene flavonone conjugate (a), fullerene dipeptide conjugates (b). Adapted from Ref. [20] and Ref. [21].

Conclusions

In summary, this Concept article overviews the key biomedical applications of fullerene monoderivatives, including cellular uptake, photosensitizer in PDT, antiviral and antibacterial behavior and ROS scavenging. Further understanding of their aggregation behavior, and the structure–property correlation pertaining to the cage functionalization, aggregation state, molecular weight, surface charge will facilitate the development of these carbon-based molecular nanomaterials as new medicines.

Conflict of Interests

The authors declare no conflict of interest.

Keywords: Fullerene monoderivatives · cellular uptake · photodynamic therapy · ROS scavenging

[1] I. Rašović, *Mater. Sci. Technol.* **2017**, *33*, 777–794.
[2] E. Castro, A. H. Garcia, G. Zavala, L. Echegoyen, *J. Mater. Chem. B* **2017**, *5*, 6523–6535.
[3] H. W. Kroto, J. R. Heath, S. C. O'Brien, R. F. Curl, R. E. Smalley, *Nature* **1985**, *318*, 162–163.
[4] L. O. Husebo, B. Sitharaman, K. Furukawa, T. Kato, L. J. Wilson, *J. Am. Chem. Soc.* **2004**, *126*, 12055–12064.
[5] Y. Zhou, J. Li, H. Ma, M. Zhen, J. Guo, L. Wang, L. Jiang, C. Shu, C. Wang, *ACS Appl. Mater. Interfaces* **2017**, *9*, 35539–35547.
[6] L. Xiao, R. Huang, Y. Zhang, T. Li, J. Dai, N. Nannapuneni, T. R. Chastanet, M. Chen, F. H. Shen, L. Jin, H. C. Dorn, X. Li, *ACS Appl. Mater. Interfaces* **2019**, *11*, 38405–38416.
[7] H. Ma, X. Zhang, Y. Yang, S. Li, J. Huo, Y. Liu, M. Guan, M. Zhen, C. Shu, J. Li, C. Wang, *Langmuir* **2021**, *37*, 2740–2748.
[8] G. Zhang, Y. Liu, D. Liang, L. Gan, Y. Li, *Angew. Chem. Int. Ed.* **2010**, *49*, 5293–5295.
[9] R. Zahran, Z. Hawash, *Adv. Mater. Interfaces* **2022**, *9*, 2201438.
[10] M. J. Siringan, A. Dawar, J. Zhang, *Mater. Chem. Front.* **2023**, 10.1039.D3QM00004D.
[11] C. J. Brabec, S. Gowrisanker, J. J. M. Halls, D. Laird, S. Jia, S. P. Williams, *Adv. Mater.* **2010**, *22*, 3839–3856.
[12] C.-Z. Li, H.-L. Yip, A. K.-Y. Jen, *J. Mater. Chem.* **2012**, *22*, 4161.
[13] L. Echegoyen, L. E. Echegoyen, *Acc. Chem. Res.* **1998**, *31*, 593–601.
[14] M. Prato, *J. Mater. Chem.* **1997**, *7*, 1097–1109.
[15] M. D. Tzirakis, M. Orfanopoulos, *Chem. Rev.* **2013**, *113*, 5262–5321.

[16] R. Sijbesma, G. Srdanov, F. Wudl, J. A. Castoro, C. Wilkins, S. H. Friedman, D. L. DeCamp, G. L. Kenyon, *J. Am. Chem. Soc.* **1993**, *115*, 6510–6512.
[17] S. H. Friedman, D. L. DeCamp, R. P. Sijbesma, G. Srdanov, F. Wudl, G. L. Kenyon, *J. Am. Chem. Soc.* **1993**, *115*, 6506–6509.
[18] R. Biswas, S. Yang, R. A. Crichton, P. Adly-Gendi, T. K. Chen, W. P. Kopcha, Z. Shi, J. Zhang, *Nanoscale* **2022**, *14*, 4456–4462.
[19] K. Liosi, A. J. Stasyuk, F. Masero, A. A. Voityuk, T. Nauser, V. Mougel, M. Solà, Y. Yamakoshi, *JACS Au* **2021**, *1*, 1601–1611.
[20] R. F. Enes, A. S. F. Farinha, A. C. Tomé, J. A. S. Cavaleiro, R. Amorati, S. Petrucci, G. F. Pedulli, *Tetrahedron* **2009**, *65*, 253–262.
[21] P.-F. Zhao, Z.-Q. Liu, *Chem. Res. Toxicol.* **2021**, *34*, 2366–2374.
[22] A. Saminathan, M. Zajac, P. Anees, Y. Krishnan, *Nat. Rev. Mater.* **2021**, DOI 10.1038/s41578-021-00396-8.
[23] S. Foley, C. Crowley, M. Smaihi, C. Bonfils, B. F. Erlanger, P. Seta, C. Larroque, *Biochem. Biophys. Res. Commun.* **2002**, *294*, 116–119.
[24] J. Yang, K. Wang, J. Driver, J. Yang, A. R. Barron, *Org. Biomol. Chem.* **2007**, *5*, 260–266.
[25] L. W. Zhang, J. Yang, A. R. Barron, N. A. Monteiro-Riviere, *Toxicol. Lett.* **2009**, *191*, 149–157.
[26] J.-H. Liu, L. Cao, P. G. Luo, S.-T. Yang, F. Lu, H. Wang, M. J. Meziani, Sk. A. Haque, Y. Liu, S. Lacher, Y.-P. Sun, *ACS Appl. Mater. Interfaces* **2010**, *2*, 1384–1389.
[27] G. E. Magoulas, M. Bantzi, D. Messari, E. Voulgari, C. Gialeli, D. Barbouri, A. Giannis, N. K. Karamanos, D. Papaioannou, K. Avgoustakis, *Pharm. Res.* **2015**, *32*, 1676–1693.
[28] J. Wang, L. Xie, T. Wang, F. Wu, J. Meng, J. Liu, H. Xu, *Acta Biomater.* **2017**, *59*, 158–169.
[29] T. Kobayashi, T. Yasuno, K. Takahashi, S. Nakamura, T. Mashino, T. Ohe, *Bioorg. Med. Chem. Lett.* **2021**, *49*, 128267.
[30] Y. Yamakoshi, N. Umezawa, A. Ryu, K. Arakane, N. Miyata, Y. Goda, T. Masumizu, T. Nagano, *J. Am. Chem. Soc.* **2003**, *125*, 12803–12809.
[31] P. Mroz, G. P. Tegos, H. Gali, T. Wharton, T. Sarna, M. R. Hamblin, *Photochem. Photobiol. Sci.* **2007**, *6*, 1139–1149.
[32] M. R. Hamblin, *Photochem. Photobiol. Sci.* **2018**, *17*, 1515–1533.
[33] D. E. J. G. J. Dolmans, D. Fukumura, R. K. Jain, *Nat. Rev. Cancer* **2003**, *3*, 380–387.
[34] M. Guan, T. Qin, J. Ge, M. Zhen, W. Xu, D. Chen, S. Li, C. Wang, H. Su, C. Shu, *J. Mater. Chem. B* **2015**, *3*, 776–783.
[35] Q. Tang, W. Xiao, J. Li, D. Chen, Y. Zhang, J. Shao, X. Dong, *J. Mater. Chem. B* **2018**, *6*, 2778–2784.
[36] E. J. Gonzalez Lopez, A. M. Sarotti, S. R. Martínez, L. P. Macor, J. E. Durantini, M. Renfige, M. A. Gervaldo, L. A. Otero, A. M. Durantini, E. N. Durantini, D. A. Heredia, *Chem. Eur. J.* **2022**, *28*, e202103884.
[37] A. Ikeda, T. Mae, M. Ueda, K. Sugikawa, H. Shigeto, H. Funabashi, A. Kuroda, M. Akiyama, *Chem. Commun.* **2017**, *53*, 2966–2969.
[38] C. R. Miller, B. Bondurant, S. D. McLean, K. A. McGovern, D. F. O'Brien, *Biochemistry* **1998**, *37*, 12875–12883.
[39] Y. Iwase, K. Nishi, J. Fujimori, T. Fukai, N. Yumita, T. Ikeda, F. Chen, Y. Momose, S. Umemura, *Jpn. J. Appl. Phys.* **2016**, *55*, 07KF02.
[40] S. Pacor, A. Grillo, L. Đorđević, S. Zorzet, M. Lucafò, T. Da Ros, M. Prato, G. Sava, *BioMed Res. Int.* **2015**, *2015*, 1–13.
[41] G. Mion, C. Mari, T. Da Ros, R. Rubbiani, G. Gasser, T. Gianferrara, *ChemistrySelect* **2017**, *2*, 190–200.
[42] C. Zhou, Q. Liu, W. Xu, C. Wang, X. Fang, *Chem. Commun.* **2011**, *47*, 2982.
[43] K. Mizuki, S. Matsumoto, T. Honda, K. Maeda, S. Toyama, D. Iohara, F. Hirayama, S. Okazaki, K. Takeshita, T. Hatta, *Chem. Pharm. Bull.* **2018**, *66*, 822–825.
[44] Y. Iwamoto, Y. Yamakoshi, *Chem. Commun.* **2006**, 4805–4807.
[45] A. Yu. Belik, A. Yu. Rybkin, N. S. Goryachev, A. P. Sadkov, N. V. Filatova, A. G. Buyanovskaya, V. N. Talanova, Z. S. Klemenkova, V. S. Romanova, M. O. Koifman, A. A. Terentiev, A. I. Kotelnikov, *Spectrochim. Acta. A. Mol. Biomol. Spectrosc.* **2021**, *260*, 119885.
[46] Q. Li, C. Liu, H. Li, *J. Nanosci. Nanotechnol.* **2016**, *16*, 5592–5597.
[47] X. Zhu, A. Quaranta, R. V. Bensasson, M. Sollogoub, Y. Zhang, *Chem. Eur. J.* **2017**, *23*, 9462–9466.
[48] J. Wang, Z. Zhang, W. Wu, X. Jiang, *Chin. J. Chem.* **2014**, *32*, 78–84.
[49] W. Shen, L. Bao, X. Lu, *Chin. J. Chem.* **2022**, *40*, 275–284.
[50] T. Li, H. C. Dorn, *Small* **2017**, *13*, 1603152.
[51] T. Wang, C. Wang, *Small* **2019**, *15*, 1901522.
[52] P. Jin, Y. Li, S. Magagula, Z. Chen, *Coord. Chem. Rev.* **2019**, *388*, 406–439.
[53] Y. Li, Y. Sun, W. P. Kopcha, J. Zhang, *Chin. J. Chem.* **2023**, *41*, 2025–2034. https://doi.org/10.1002/cjoc.202300051.
[54] Y. Li, R. Biswas, W. P. Kopcha, T. Dubroca, L. Abella, Y. Sun, R. A. Crichton, C. Rathnam, L. Yang, Y.-W. Yeh, K. Kundu, A. Rodríguez-Fortea, J. M. Poblet, K.-B. Lee, S. Hill, J. Zhang, *Angew. Chem. Int. Ed.* **2023**, *62*, e202211704.
[55] S. Aroua, W. B. Schweizer, Y. Yamakoshi, *Org. Lett.* **2014**, *16*, 1688–1691.
[56] P. Piotrowski, K. Klimek, G. Ginalska, A. Kaim, *Materials* **2021**, *14*, 1566.
[57] T. Yasuno, T. Ohe, K. Takahashi, S. Nakamura, T. Mashino, *Bioorg. Med. Chem. Lett.* **2015**, *25*, 3226–3229.
[58] T. A. Strom, S. Durdagi, S. S. Ersoz, R. E. Salmas, C. T. Supuran, A. R. Barron, *J. Pept. Sci.* **2015**, *21*, 862–870.
[59] M. Brettreich, A. Hirsch, *Tetrahedron Lett.* **1998**, *39*, 2731–2734.
[60] A. Muñoz, B. M. Illescas, J. Luczkowiak, F. Lasala, R. Ribeiro-Viana, J. Rojo, R. Delgado, N. Martín, *J. Mater. Chem. B* **2017**, *5*, 6566–6571.
[61] Q. Chen, Z. Ma, G. Liu, H. Wei, X. Xie, *Digest J. Nanomat. Biostruct.* **2016**, *11*(3), 753–761.
[62] S. Tollas, I. Bereczki, A. Sipos, E. Rőth, G. Batta, L. Daróczi, S. Kéki, E. Ostorházi, F. Rozgonyi, P. Herczegh, *Eur. J. Med. Chem.* **2012**, *54*, 943–948.
[63] Z. Markovic, V. Trajkovic, *Biomaterials* **2008**, *29*, 3561–3573.
[64] M. J. Akhtar, M. Ahamed, H. A. Alhadlaq, A. Alshamsan, *Biochim. Biophys. Acta Gen. Subj.* **2017**, *1861*, 802–813.
[65] J.-J. Yin, F. Lao, P. P. Fu, W. G. Wamer, Y. Zhao, P. C. Wang, Y. Qiu, B. Sun, G. Xing, J. Dong, X.-J. Liang, C. Chen, *Biomaterials* **2009**, *30*, 611–621.
[66] H. Ma, J. Zhao, H. Meng, D. Hu, Y. Zhou, X. Zhang, C. Wang, J. Li, J. Yuan, Y. Wei, *ACS Appl. Mater. Interfaces* **2020**, *12*, 16104–16113.
[67] T. Li, L. Xiao, J. Yang, M. Ding, Z. Zhou, L. LaConte, L. Jin, H. C. Dorn, X. Li, *ACS Appl. Mater. Interfaces* **2017**, *9*, 17681–17687.
[68] M. Chen, S. Zhou, L. Guo, L. Wang, F. Yao, Y. Hu, H. Li, J. Hao, *Langmuir* **2019**, *35*, 6939–6949.

Manuscript received: June 7, 2023
Revised manuscript received: August 30, 2023
Version of record online: September 20, 2023